# Chimeras on a ring of oscillator populations

Carlo R. Laing[a)]

(Dated: 19 December 2022)

Chimeras occur in networks of coupled oscillators and are characterised by coexisting groups of synchronous oscillators and asynchronous oscillators. We consider a network formed from $N$ equal-sized populations, at equally-spaced points around a ring. We use the Ott/Antonsen ansatz to derive coupled ODEs governing the level of synchrony within each population, and describe chimeras using a self-consistency argument. For $N = 2$ and 3, our results are compared with previously known ones. We obtain new results for the cases of $4, 5, \ldots, 12$ populations, and a numerically based conjecture resulting from the behaviour of larger numbers of populations. We find macroscopic chaos when more than five populations are considered, but conjecture that this behaviour vanishes as the number of populations is increased.

[a)]School of Mathematical and Computational Sciences, Massey University, Private Bag 102-904 North Shore Mail Centre, Auckland, New Zealand. c.r.laing@massey.ac.nz

**Chimeras are spatiotemporal patterns of varying synchrony which occur in networks of coupled oscillators. We consider a network formed from $N$ populations of oscillators, with nonlocal coupling between the populations, whose strength depends on the distance between them. The cases of $N = 2, 3$ and $N = \infty$ have been studied previously, and we bridge the gap between these two extremes. We investigate the effects of varying both $N$ and the level of frequency heterogeneity within the populations. We find chaotic behaviour for sufficiently large $N$, but this behaviour vanishes as $N \to \infty$. Also, for finite $N$ and sufficiently small frequency heterogeneity, stationary chimeras are found to be unstable.**

---

## I. INTRODUCTION

Chimeras occur in networks of coupled oscillators and are characterised by coexisting groups (or domains) of synchronous oscillators and asynchronous oscillators[21,25]. One of the earliest systems in which such a state was observed is a ring of nonlocally coupled phase oscillators[2,3,13]. Here, oscillators on part of the ring are synchronous while those on the remainder of the ring are not. To analyse this behaviour, Abrams et al.[1] coarse-grained the domain into two equally-sized populations of oscillators, with strong coupling within a population and weaker coupling between populations. Here, in the limit of an infinite number of oscillators in each population, a chimera appears as a state in which one population is perfectly synchronised while the other is partially synchronous. These authors used the Ott/Antonsen ansatz[23,24] to derive differential equations governing the complex-valued order parameters describing the levels of synchrony within the two populations. The only work which addresses the intermediate case of coarse-graining a ring to more than two populations seems to be that of Martens[19], who considered three populations. He found two types of chimeras, with either one or two populations being synchronous while the other two (one) were partially synchronous. Martens also used the Ott/Antonsen ansatz to study these chimeras, as many have done subsequently in different settings[15,16,18,21,31,35]. No coarse-graining into more than three populations seems to have been done, and Martens raised a number of questions about what would happen if this was undertaken. For example, would the number of possible chimera states increase as the number of populations is increased, with every possible combination of synchronous and asynchronous populations allowed?

Another result of interest is that of[34], who showed that while for an infinite number of identical

phase oscillators on a ring a chimera is a neutrally stable stationary pattern, numerical simulations of finite networks show that chimeras move in an irregular way about the domain and eventually collapse, with an average lifetime which increases exponentially with network size. The irregular motion was shown to be chaotic, and the collapse was to the completely synchronous state. However, for networks formed of two populations each consisting of between two and an infinite number of oscillators, Panaggio et al.[26] showed that chimeras are stable and not chaotic. This raises the question of the origin of the chaotic behaviour observed in[34], since it does not occur for networks of either two populations, or an infinite number of them (each consisting of one oscillator), but for a finite number of populations (each consisting of one oscillator).

In this paper we address some of the questions raised above by considering a ring of sinusoidally coupled phase oscillator populations, with each population being at one of a number of equally-spaced points around the ring. We let the number of oscillators in each population be infinite. The oscillators are chosen to be heterogeneous, so that the Ott/Antonsen manifold is attracting rather than neutrally stable, and the level of heterogeneity is a key parameter which is varied. For the cases of two or three populations, our results can be compared with previously known ones. We obtain new results for the cases of $4,5,\ldots,12$ populations, and a numerically based conjecture resulting from the behaviour of larger numbers of populations. We find macroscopic chaos when more than five populations are considered, but conjecture that this behaviour vanishes as the number of populations is increased. The model is presented in Sec. II and we also characterise the possible solutions of interest there. Results are given in Sec. III and we conclude in Sec. IV.

## II. MODEL

The model consists of $N$ populations each consisting of $M$ oscillators. The populations are thought of as being at the vertices of a regular $N$-gon, which lie on a circle $S$ with circumference $2\pi$. The strength of coupling between two oscillators depends only on which populations they are in, and the (positive) strength of coupling between populations decays as the distance between them (the shortest distance on $S$) increases.

The equations are

$$\frac{d\theta_k^a}{dt} = \omega_k^a + \frac{1}{M}\sum_{b=1}^{N}\sum_{j=1}^{M} C_{a,b}\sin\left(\theta_j^b - \theta_k^a - \alpha\right) \tag{1}$$

where $\theta_k^a$ is the phase of the $k$th oscillator in population $a$. For all $a \in \{1,2,\ldots N\}$ and all $k \in \{1,2,\ldots M\}$, $\omega_k^a$ is chosen from a Lorentzian with centre zero and half-width-at-half maximum $\delta$. Such a model was presented in[27], although they considered identical oscillators within each population, and possibly different values of $\omega^a$ for each population, and left the coupling between populations to be general. Skardal and Restrepo[29] considered a similar model with $\alpha = 0$ and a network for which coupling within a population was strong while that between oscillators in different populations was uniform and weak. Smirnov et al.[30] considered a model of this form for which coupling was only between neighbouring populations. See also[5].

$C$ is an $N \times N$ coupling matrix which is circulant, i.e. fully determined once a row is specified. To calculate $C$, let $g(x) = (1 + B\cos x)/(2\pi)$ where $B$ is a parameter and $x$ is a position on $S$. Let $\Delta x = 2\pi/N$ be the arclength on $S$ between populations, and $x_i = (i-1)\Delta x$ be the locations of the populations, for $i = 1,2,\ldots N$. The entries of $C$ are formed by integrating $g(x)$ over intervals of length $\Delta x$, centred at the $x_i$. Specifically, entries in the first row of $C$ are

$$C_{1,i} = \int_{x_i-\Delta x/2}^{x_i+\Delta x/2} g(x)\,dx = \frac{1}{N} + B\frac{\sin(x_i+\Delta x/2) - \sin(x_i-\Delta x/2)}{2\pi} = \frac{1}{N} + B\frac{\sin(\Delta x/2)\cos(x_i)}{\pi} \quad (2)$$

and thus

$$C_{a,b} = \frac{1}{N} + \frac{B\sin(\Delta x/2)}{\pi}\cos(x_a - x_b) \quad (3)$$

Entries in $C_{1,i}$ for $N = 2,3,4,20$ and $B = 0.35$ are shown in Fig. 1. We see that $C_{1,1}$ is always the largest, i.e. coupling within a population is stronger than between populations. The coupling strength between populations decreases as the distance between them (measured along the shortest path on $S$ connecting them) increases, reaching a minimum for populations most distant from one another. We fix $B = 0.35$ for the rest of the paper.

### A. $M = \infty$ equations

Letting the number of oscillators in a population, $M$, go to infinity, and using the Ott/Antonsen ansatz we find that the dynamics of the populations are given by

$$\frac{dz_a}{dt} = -\delta z_a + (i/2)\left[e^{-i\beta}R_a + e^{i\beta}\bar{R}_a z_a^2\right] \quad (4)$$

where $\beta = \pi/2 - \alpha$, overline indicates the complex conjugate, and

$$R_a = \sum_{b=1}^{N} C_{a,b} z_b \quad (5)$$

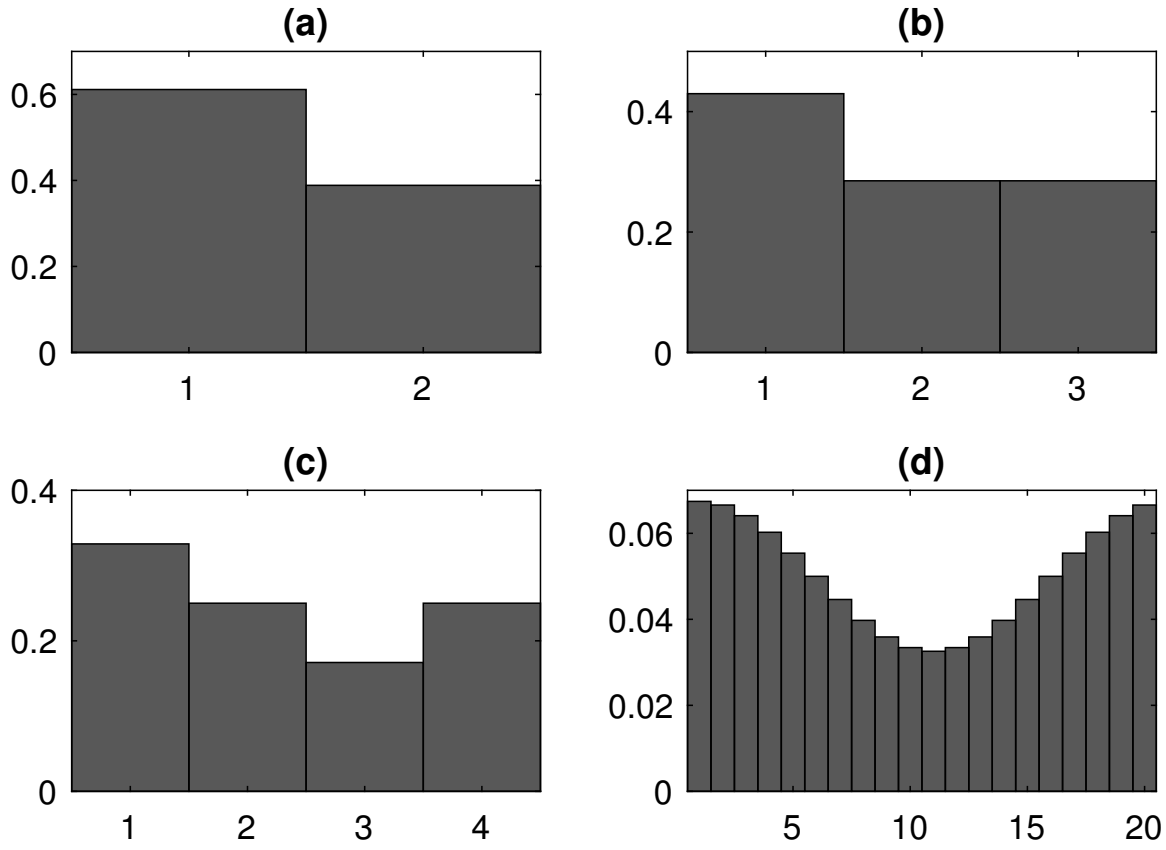


FIG. 1. Entries in the first row of the coupling matrix, $C_{1,i}$ for $N = 2,3,4,20$ ((a),(b),(c) and (d), respectively). In each panel the horizontal index is $i$. Parameter: $B = 0.35$.

(A derivation of similar equations is given in[4,18].) The complex-valued order parameter $z_a$ is the average over $k$ of $e^{i\theta_k^a}$ for oscillators in population $a$. Its magnitude describes the level of synchrony within population $a$ while the negative of its argument gives the mean of the phases within population $a$[1,15]. Specifically, if $z_a = r_a e^{-i\phi_a}$ then the phase distribution for oscillators in population $a$ is

$$F_a(\theta) = \frac{1 - r_a^2}{2\pi[1 - 2r_a \cos(\theta - \phi_a) + r_a^2]}, \tag{6}$$

a unimodal function with its maximum at $\theta = \phi_a$.

Note that if we considered identical oscillators (i.e. $\delta = 0$) each population would be described by a complex-valued equation similar to (4) and another real-valued differential equation, and a number of constants would have to be specified for each population[27]; this is the case for either finite or infinite $M$ — see the Watanabe/Strogatz ansatz[28,32]. Note also that as $N \to \infty$, $C_{a,b} \to$

$(1+B\cos(x_a-x_b))/N = g(x_a-x_b)\Delta x$, so in this limit we have

$$R(x,t) = \int_0^{2\pi} g(x-y)z(y,t)\,dy \tag{7}$$

and the dynamics are given by

$$\frac{\partial z(x,t)}{\partial t} = -\delta z(x,t) + (i/2)\left[e^{-i\beta}R(x,t) + e^{i\beta}\bar{R}(x,t)z^2(x,t)\right] \tag{8}$$

a system studied in[2,3,15,22].

Note that (4) is invariant under the rotation $z_a \to z_a e^{i\gamma}$ for all $a$ and any constant $\gamma$, so to remove this degeneracy we first write $z_a = r_a e^{i\phi_a}$ and thus have the dynamics

$$\dot{r}_a = -\delta r_a + \frac{r_a^2-1}{2}\sum_{b=1}^{N} C_{a,b} r_b \sin(\phi_b - \phi_a - \beta) \tag{9}$$

and

$$\dot{\phi}_a = \frac{1+r_a^2}{2r_a}\sum_{b=1}^{N} C_{a,b} r_b \cos(\phi_b - \phi_a - \beta) \tag{10}$$

The degeneracy means that only phase differences appear in these equations (as in (1)), and thus to remove it we define phase difference variables relative to $\phi_N$: $\psi_a \equiv \phi_a - \phi_N$ for $a = 1,2\ldots N-1$. Thus we have the $2N-1$ equations

$$\dot{r}_a = -\delta r_a + \frac{r_a^2-1}{2}\sum_{j=1}^{N} C_{a,b} r_b \sin(\psi_b - \psi_a - \beta) \tag{11}$$

for $a = 1,2\ldots N$ and

$$\dot{\psi}_a = \frac{1+r_a^2}{2r_a}\sum_{b=1}^{N} C_{a,b} r_b \cos(\psi_b - \psi_a - \beta) - \frac{1+r_N^2}{2r_N}\sum_{b=1}^{N} C_{N,b} r_b \cos(\psi_b - \beta) \tag{12}$$

for $a = 1,2\ldots N-1$, where $\psi_N$ is set to zero.

### B. Steady states via self-consistency

The steady states we are interested in are stationary solutions of (4) in a rotating coordinate frame[21], i.e. they satisfy

$$0 = (i\omega - \delta)z_a + (i/2)\left[e^{-i\beta}R_a + e^{i\beta}\bar{R}_a z_a^2\right] \tag{13}$$

for $a = 1,2,\ldots N$ where $\omega$ is the rate at which the coordinate frame is rotating. Solving this for $z_a$ we obtain

$$z_a = f(R_a) \equiv \frac{\delta - i\omega - \sqrt{(i\omega-\delta)^2 + |R_a|^2}}{ie^{i\beta}\bar{R}_a} \tag{14}$$

where we take the negative square root to ensure $|z_a| \leq 1$ and we can insert this into (5) to obtain a set of equations that the $R_a$ must satisfy:

$$R_a = \sum_{b=1}^{N} C_{a,b} \left( \frac{\delta - i\omega - \sqrt{(i\omega - \delta)^2 + |R_b|^2}}{ie^{i\beta}\bar{R}_b} \right) \tag{15}$$

Using the form of $C_{a,b}$ we have

$$R_a = \frac{1}{N}\sum_{b=1}^{N} f(R_b) + \frac{B\sin(\Delta x/2)}{\pi}\left[\cos(x_a)\sum_{b=1}^{N}\cos(x_b)f(R_b) + \sin(x_a)\sum_{b=1}^{N}\sin(x_b)f(R_b)\right] \tag{16}$$

i.e. each $R_a$ has the form

$$R_a = D + E\cos(x_a) + F\sin(x_a) \tag{17}$$

for some constants $D, E$ and $F$. (These are independent of index $a$.) We can use the invariance under rotation to assume that $D$ is real and positive, but $E$ and $F$ are generically complex.

The network has the symmetry of a regular $N$-gon, so given a steady state, we can obtain another one by rotating it through a multiple of $2\pi/N$ around the circle $S$, i.e. increasing (or decreasing) all population indices by the same amount. For odd $N$ the only steady states found below were invariant under reflection in a line passing through one population and the centre of $S$. These can be described by (17) with $F = 0$. Thus summing (17) over $a$ and using (15) we obtain

$$D = \frac{1}{N}\sum_{a=1}^{N}\sum_{b=1}^{N} C_{a,b}\left( \frac{\delta - i\omega - \sqrt{(i\omega - \delta)^2 + |D + E\cos(x_b)|^2}}{ie^{i\beta}(D + \bar{E}\cos(x_b))} \right). \tag{18}$$

Multiplying (17) by $\cos(x_a)$ and then summing over $a$ we obtain

$$E = \frac{2}{N}\sum_{a=1}^{N}\sum_{b=1}^{N} C_{a,b}\left( \frac{\delta - i\omega - \sqrt{(i\omega - \delta)^2 + |D + E\cos(x_b)|^2}}{ie^{i\beta}(D + \bar{E}\cos(x_b))} \right)\cos(x_a). \tag{19}$$

Taking real and imaginary parts of (18)-(19) gives four real equations for the four unknowns: $D, \omega, \mathrm{Re}(E), \mathrm{Im}(E)$.

For even $N$ we saw two types of steady states: those invariant under reflection in a line passing through one population and the centre of $S$ (and thus the population on the opposite side), and those invariant under reflection in a line through the centre of $S$ which evenly divides the network into two groups of $N/2$ populations. The former type can be found as above. The latter have the form $R_a = D + E\cos(x_a + \Delta x/2)$. Summing this expression over $a$ we obtain

$$D = \frac{1}{N}\sum_{a=1}^{N}\sum_{b=1}^{N} C_{a,b}\left( \frac{\delta - i\omega - \sqrt{(i\omega - \delta)^2 + |D + E\cos(x_b + \Delta x/2)|^2}}{ie^{i\beta}(D + \bar{E}\cos(x_b + \Delta x/2))} \right) \tag{20}$$

and by using similar reasoning to that above we obtain

$$E=\frac{2}{N}\sum_{a=1}^{N}\sum_{b=1}^{N}C_{a,b}\left(\frac{\delta-i\omega-\sqrt{(i\omega-\delta)^2+|D+E\cos(x_b+\Delta x/2)|^2}}{ie^{i\beta}(D+\bar{E}\cos(x_b+\Delta x/2))}\right)\cos(x_a+\Delta x/2). \quad (21)$$

Taking real and imaginary parts of (20)-(21) enables us to find $D,\omega,\mathrm{Re}(E),\mathrm{Im}(E)$ for these types of solution. Similar self-consistency equations have been derived previously[3,14].

In summary, all of the steady states of interest can be found by solving four simultaneous nonlinear equations for $D,\omega,\mathrm{Re}(E),\mathrm{Im}(E)$, substituting these into the appropriate expression for $R_a$, which then gives the $z_a$ from (14). These can then be uniformly rotated if necessary to make $z_N$ real, and thus we have values of the variables needed for (11)-(12). We see that there are spatially uniform states with $E=0$, and states with $E\neq 0$ for which both the real and imaginary parts of the vector $R$ (with components $R_a$) vary sinusoidally as we move around the circle $S$. Thus for the type of coupling used here, one cannot obtain stationary chimeras with arbitrary levels of synchrony in different populations, only those described here.

## III. RESULTS

We now show the results of numerically analysing (11)-(12) for $2\leq N\leq 12$ and for fixed parameter values $B=0.35$ and $\beta=0.03$.

### A. Dynamics for small $N$

#### *1.* $N=2$

This case has been studied by a number of authors[20]. The entries of the first row of the coupling matrix are

$$C_{1,1}=1/2+0.35/\pi \qquad \text{and} \qquad C_{1,2}=1/2-0.35/\pi \quad (22)$$

A parameter $A$ is used in[1,12,14,16,26] to quantify the difference between coupling within a population and coupling between populations, and we see that the values above correspond to $A=C_{1,1}-C_{1,2}=0.7/\pi\approx 0.2228$. The ref.[1,26] considered the case of $\delta=0$, i.e. identical oscillators, while[12,14,16] considered $\delta>0$ and performed some bifurcation analysis as $\delta$ was varied. The papers[1,26] show that for $(A,\beta)=(0.2228,0.03)$ and $\delta=0$ the system supports a stable stationary chimera, i.e. a solution for which $|z_1|=1$ and $|z_2|<1$ (or vice versa). For other values of $A$ and $\beta$,

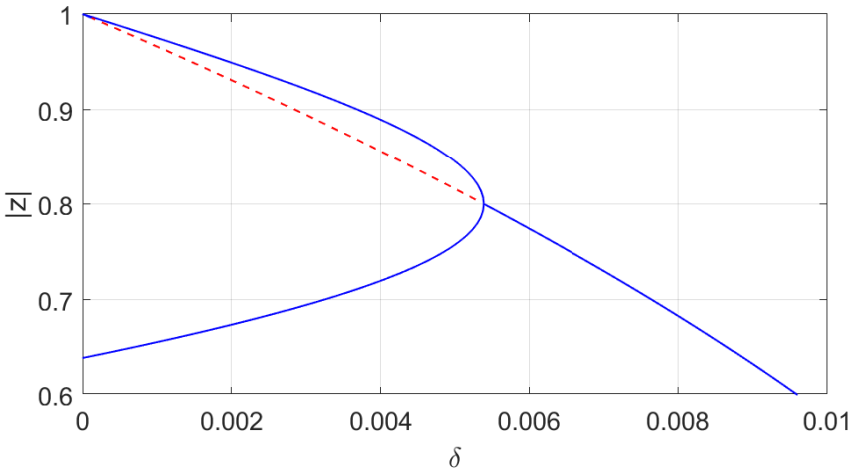


FIG. 2. $N = 2$. Blue: stable steady state; red: unstable steady state. The stable chimeras which exists at $\delta = 0$ are destroyed in a pitchfork bifurcation as $\delta$ is increased. The equally-synchronous state for which $|z_1| = |z_2|$ is stable for $0 \leq \delta < 0.000123$ (barely visible) and for $0.005155 < \delta$.

refs.[12,14,16] show that increasing $\delta$ causes the values of $|z_1|$ and $|z_2|$ to approach one another until they meet in a pitchfork bifurcation, destroying the chimeras, beyond which only solutions with $|z_1| = |z_2|$ are stable. The results of calculations for $(B,\beta) = (0.35, 0.03)$ are shown in Fig. 2 and we see that the same scenario occurs here. $|z|$ at steady states is shown for both populations and we see the stable chimera destroyed in a pitchfork bifurcation as $\delta$ is increased. The completely synchronous state for which $|z_1 = |z_2| = 1$ is stable for $\delta = 0$ and persists as $\delta$ is increased, (and the $|z_a|$ decrease) but loses stability at $\delta \approx 0.000123$ before regaining stability at $\delta \approx 0.005155$.

### *2.* $N = 3$

The $N = 3$ case was considered by Martens[19] who used a coupling matrix of the form

$$\begin{pmatrix} 1 & 1-A & 1-A \\ 1-A & 1 & 1-A \\ 1-A & 1-A & 1 \end{pmatrix}. \tag{23}$$

For our system

$$C_{1,1} = \frac{1}{3} + \frac{0.35\sqrt{3}}{2\pi} \approx 0.4298 \qquad \text{and} \qquad C_{1,2} = C_{1,3} = \frac{1}{3} - \frac{0.35\sqrt{3}}{4\pi} \approx 0.2851 \tag{24}$$

Martens considered the case of identical oscillators, so to compare our system with his we can set $\delta = 0$ and rescale time so that $C_{1,1} = 1$. This gives a value of

$$A = 1 - \frac{\frac{1}{3} - \frac{0.35\sqrt{3}}{4\pi}}{\frac{1}{3} + \frac{0.35\sqrt{3}}{2\pi}} \approx 0.3367. \tag{25}$$

For $N = 3$ and identical oscillators we expect two types of stationary chimeras: either two populations are synchronised and one is not, or one is synchronised while two are not; see Sec. II B. Martens referred to these as SDS and DSD respectively (S for synchrony and D for drift/desynchrony). Since we will consider chimeras in networks of more than three populations we introduce the terminology of type 1 (T1) and type 2 (T2) solutions for which either one or two, respectively, populations are most synchronous. Thus a DSD solution is T1 and a SDS solution is T2. For odd $N$, a T1 solution will have two populations with the least amount of synchrony (measured by the magnitude of the $z_k$) on the opposite side of the ring from the most synchronous population, while a T2 solution will have only one least synchronous population. For even $N$ a T1 solution will have one population with the least amount of synchrony, and a T2 solution will have two. See Fig. 5 for examples of these types of solution for $N = 4$. As $N$ increases the distinction between the two types of solution becomes less relevant.

Martens analysed the T1 and T2 solutions by assuming that the synchronised population(s) had $|z_k| = 1$ and that the populations in the same state had identical dynamics, thus reducing the dynamics of the whole network to those of two variables: the magnitude of $z$ for the desynchronised population(s) and the phase difference between a synchronous population and a desynchronous one. This analysis showed that both a T1 and T2 solution were stable for the parameters above, under the assumptions above. We now show the results of analysing the full equations (11)-(12), varying $\delta$.

Fig. 3(a) shows the results for a T1 solution. For $\delta = 10^{-3}$ this stationary solution is stable and two different values of $|z|$ are seen, but as $\delta$ is decreased the solution loses stability in a supercritical Hopf bifurcation, creating a periodic solution. The maximum and minimum over one period of $|z|$ for one of the desynchronised populations is shown with crosses in Fig. 3(a). ($|z|$ for the nearly-synchronous population also varies periodically, but this is not shown, for clarity). On this periodic solution the levels of synchrony in the two desynchronised populations alternate, being half a period out of phase with one another. Decreasing $\delta$ even further, the periodic solution undergoes a Neimark–Sacker bifurcation, creating a stable quasiperiodic solution (not shown in Fig. 3(a)). Thus for infinite populations with weak (or zero) heterogeneity, the stationary T1 solution is not

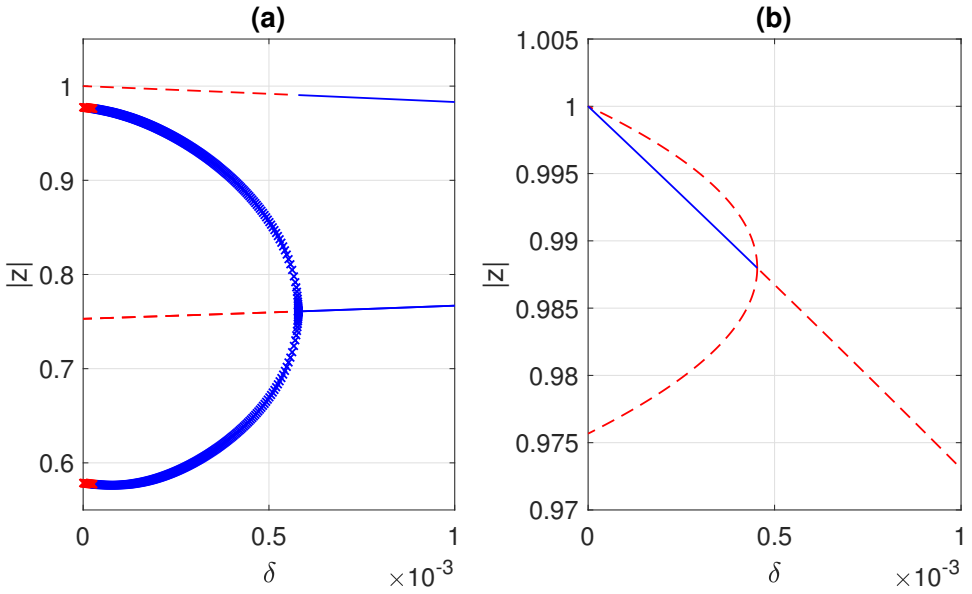


FIG. 3. $N = 3$. Blue: stable; red: unstable. Solid and dashed lines are for a fixed point, crosses show the maximum and minimum over one period of a periodic orbit, for one population. (a): T1 solution. (b): T2 solution. See text for further explanation.

actually stable. Martens[19] did report the existence of a T1 chimera in the original model (1) using identical oscillators for parameter values close to those used here, using populations of size $M = 40$.

We now consider the T2 solution, whose behaviour is shown in Fig. 3(b), where we plot $|z|$ for the two most synchronous solutions. The T2 solution is stable only for small $\delta$, where it coexists with two unstable chimeras for which the levels of synchrony in the two most synchronous solutions are slightly different. The symmetric T2 solution loses stability in a subcritical pitchfork bifurcation as $\delta$ is increased.

### *3.* $N = 4$

The results for $N = 4$ are shown in Fig. 4, with panel (a) showing the T1 solution and panel (b) the T2. Fig. 5 shows the phase distributions for both types of solution at $\delta = 10^{-3}$, for which both are stable stationary solutions. As $\delta$ is decreased the T1 solution undergoes a supercritical Hopf bifurcation, and the stable periodic orbit created in this bifurcation then loses stability through a Neimark–Sacker bifurcation as $\delta$ is decreased further. This is the same scenario as for the T1

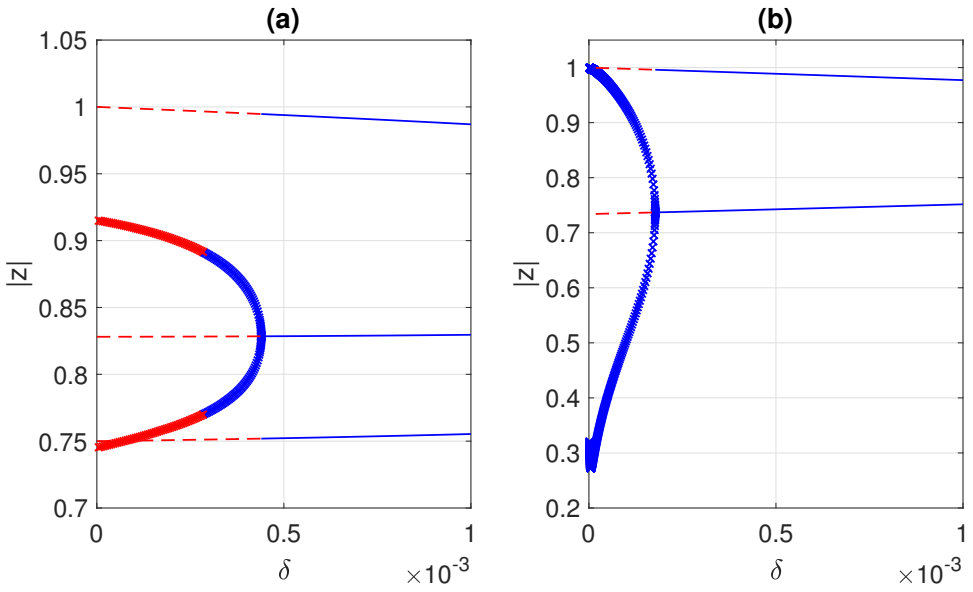


FIG. 4. $N = 4$. Blue: stable; red: unstable. Solid and dashed lines are for a fixed point, crosses show the maximum and minimum over one period of a periodic orbit for one population. (a): T1 solution. (b): T2 solution. See text for further explanation.

chimera with $N = 3$. To show the periodic orbit the maximum and minimum over one period of $|z|$ for only one of the moderately synchronous populations is shown. The T2 solution also undergoes a supercritical Hopf bifurcation as $\delta$ is decreased, and the periodic orbit created is stable down to $\delta = 0$. The maximum and minimum over one period of $|z|$ for one of the desynchronised populations is shown in Fig. 4(b).

Fig. 6 shows time series of the $|z_a|$ for both of the solutions shown in Fig. 4 for (different) values of $\delta$ for which a periodic chimera is stable. For the T1 solution, we see from Fig. 6A that the levels of synchrony within the two moderately synchronous populations ((a) and (c)) alternate, while those in the other two populations oscillate at twice this frequency. Such a solution has a spatio-temporal symmetry and is mapped to itself under a time shift of half a period followed by the interchange of populations (a) and (c). For the T2 solution, we see from Fig. 6B that the levels of synchrony within the two moderately synchronous populations ((g) and (h)) alternate, as do those in the two almost synchronous populations (although to a much lesser extent). Such a solution has a spatio-temporal symmetry and is mapped to itself under a time shift of half a period followed by exchanging populations (e) and (h) with (f) and (g), respectively.

Thus for $N = 4$, for the parameter values chosen, there are no stable stationary chimeras for

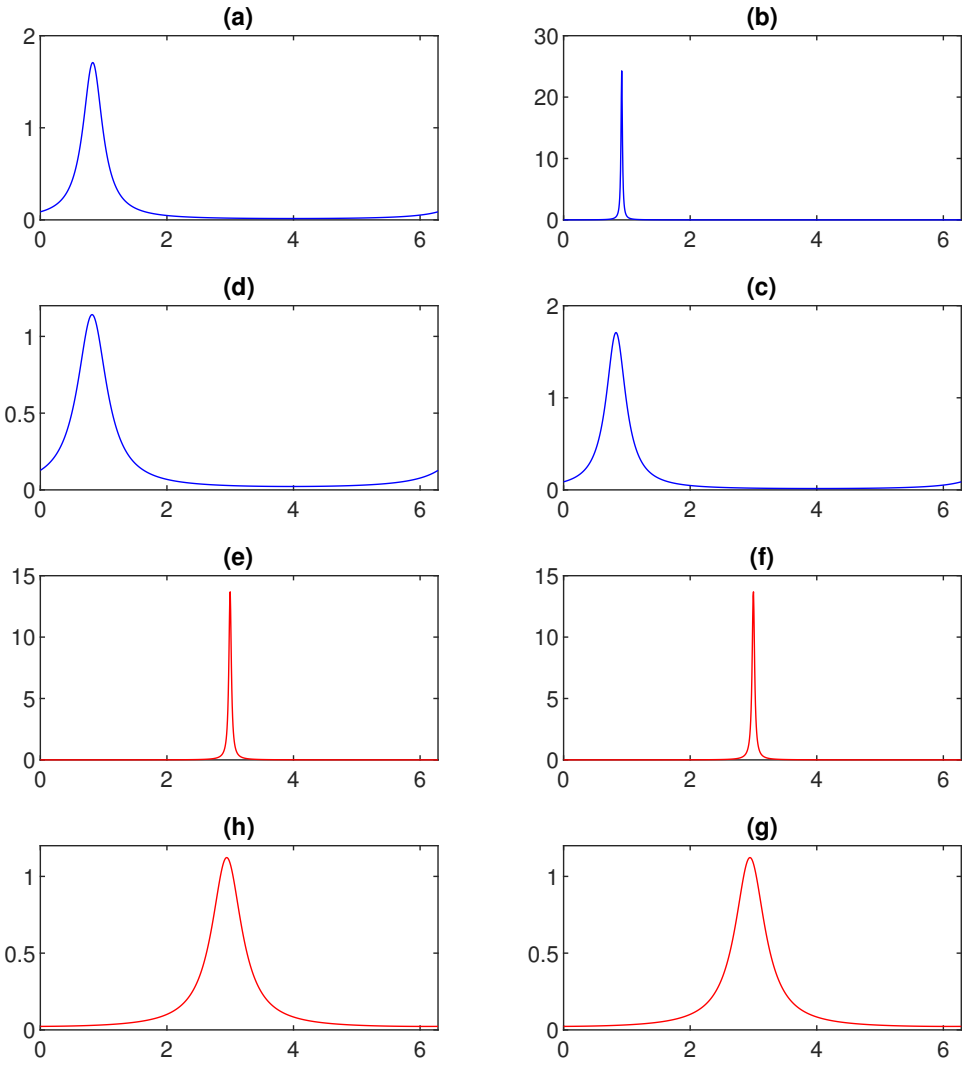


FIG. 5. Snapshots of phase densities calculated from (6) for the two types of stationary chimeras shown in Fig. 4 for $\delta = 10^{-3}$. Each panel has $\theta$ on the horizontal axis and $F_a(\theta)$ on the vertical. Panels (a),(b),(c) and (d) are for the T1 solution, and the order around the ring of populations is (a),(b),(c),(d). Population (b) is most synchronous while population (d) is least. Panels (e),(f),(g) and (h) are for the T2 solution, and the order around the ring of populations is (e),(f),(g),(h). Populations (e) and (f) are equally-synchronous, as are populations (g) and (h). The colours distinguish the two types of solution.

small levels of heterogeneity.

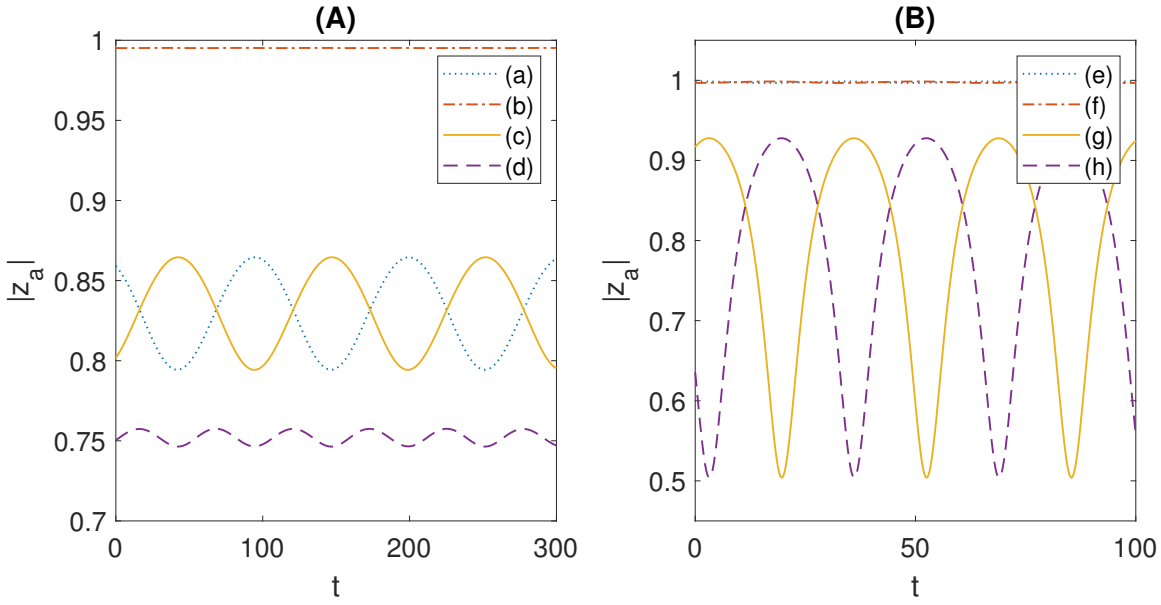


FIG. 6. $N = 4$. Time series of the $|z_a|$ (giving the instantaneous level of synchrony within a population) for a T1 solution at $\delta = 0.4 \times 10^{-3}$ (panel (A)) and for a T2 solution at $\delta = 0.1 \times 10^{-3}$ (panel (B)). The labelling of the populations corresponds to those in Fig. 5.

### *4.* $N = 5$

The T1 solution is stable for $\delta = 3 \times 10^{-3}$ but loses stability at $\delta \approx 2.7 \times 10^{-3}$ in what seems to be a subcritical pitchfork bifurcation. We concentrate on solutions which are stable for $0 \leq \delta \leq 10^{-3}$, so do not consider this solution further. The behaviour of the T2 solution is shown in Fig. 7. This solution also becomes unstable through a supercritical Hopf bifurcation as $\delta$ is decreased, creating a periodic orbit which then loses stability through a Neimark-Sacker bifurcation.

### *5.* $N = 6$

A T1 solution was found using the self-consistency approach in Sec. II B but this solution was found to be unstable for all values of $\delta$ for which it existed. The dynamics of the T2 solution are shown in Fig. 8. As above, the solution goes unstable in a supercritical Hopf bifurcation. However, the stable periodic orbit created there now becomes unstable in a period-doubling bifurcation as $\delta$ is decreased. The maximum and minimum over one period of $|z|$ for one of the least synchronised populations is shown in Fig. 8.

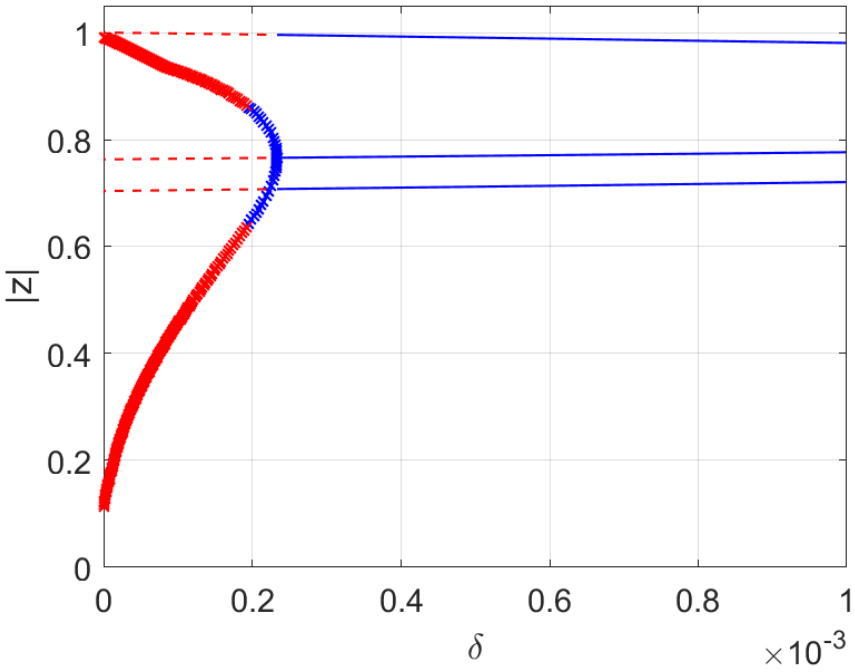


FIG. 7. $N = 5$. T2 solution. Blue: stable; red: unstable. Solid and dashed lines are for a fixed point, crosses show the maximum and minimum over one period of a periodic orbit for one population. See text for further explanation.

Fig. 9 shows the period-doubling in more detail. Here we plot maximum and minimum values of $|z|$ during a time period after which transients have decayed, for one of the least synchronised populations, as $\delta$ is varied. For $\delta = 3 \times 10^{-4}$ a stationary chimera is stable, hence all of the values shown are the same. The Hopf bifurcation shown in Fig. 8 is seen at $\delta \approx 2.7 \times 10^{-4}$ and period-doubling at $\delta \approx 2.4 \times 10^{-4}$. There seems to be a bifurcation to a quasiperiodic solution which finally becomes chaotic at $\delta \approx 1.8 \times 10^{-4}$.

The chaotic nature is shown by the largest Lyapunov exponent being positive: see Fig. 10(a). A typical chaotic solution is shown in Fig. 10(b), where the $|z_k|$ are plotted in colour. A value close to 1 indicates a synchronous population while a value significantly less than 1 indicates a partially synchronous population. The position of the synchronous population(s) moves in a seemingly random fashion, and such a solution was observed to persist for $10^6$ time units, not collapsing to the equally-synchronous state even though is stable for this value of $\delta$. This behaviour is in contrast to chimeras observed in[34], which had a finite lifetime scaling as $e^{\kappa N}$ for some constant $\kappa$.

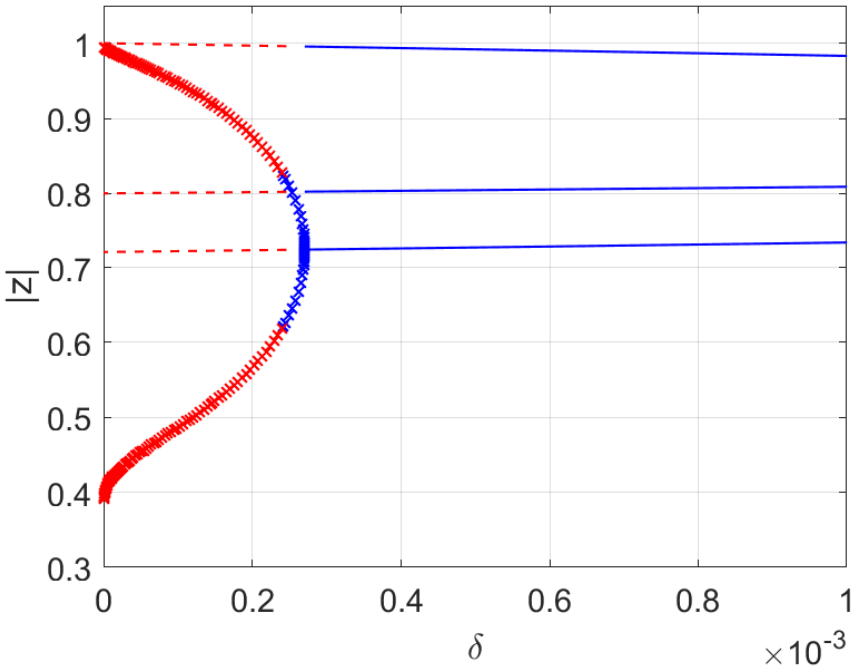


FIG. 8. $N = 6$. T2 solution. Blue: stable; red: unstable. Solid and dashed lines are for a fixed point, crosses show the maximum and minimum over one period of a periodic orbit for one of the least synchronised populations. See text for further explanation.

However, the two cases cannot be compared directly, since here we consider infinite populations of heterogeneous oscillators while[34] effectively considered the case of populations consisting of one identical oscillator.

### *6.* $N = 7$ *to* 12

A summary of the dynamics for $N = 7$ to 12 is as follows:

$N = 7$: A T1 solution was found using the self-consistency approach in Sec. II B but this solution was found to be unstable for all values of $\delta$ for which it existed. The T2 solution undergoes the same bifurcations as that for $N = 6$ (see Fig. 8) and also becomes chaotic as $\delta$ is decreased.

$N = 8$ : as with $N = 6$, a T1 solution was found using the self-consistency approach but it was always unstable. The T2 solution undergoes the same bifurcations as that for $N = 6$ (see

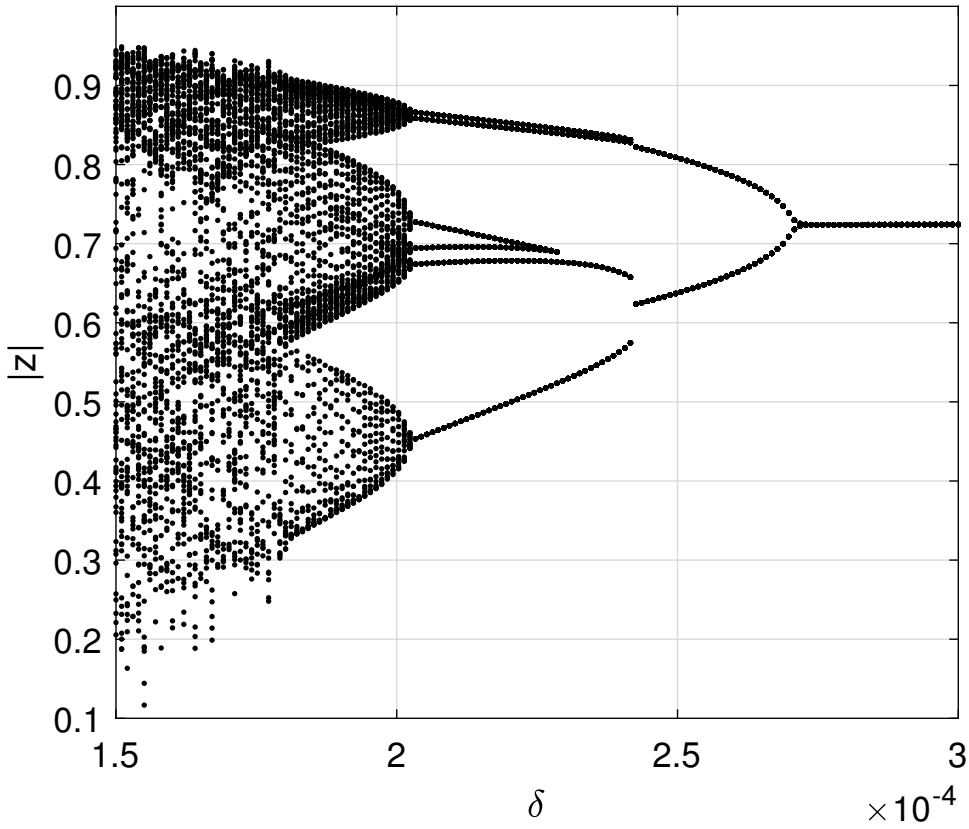


FIG. 9. $N = 6$. T2 solution. Points show the maximum and minimum of $|z|$ for one of the least synchronised populations. Compare with Fig. 8.

Fig. 8) and also becomes chaotic as $\delta$ is decreased.

$N = 9$ : a T1 solution is stable only for $0.00031 < \delta < 0.00097$. The T2 solution undergoes the same bifurcations as that for $N = 6$ (see Fig. 8) and also becomes chaotic as $\delta$ is decreased.

$N = 10$ : The T2 solution is not stable for $\delta < 10^{-3}$. The T1 solution undergoes the same bifurcations as that for T2 solution for $N = 6$ (see Fig. 8) and becomes chaotic as $\delta$ is decreased.

$N = 11$ : same as for $N = 10$.

$N = 12$ : same as for $N = 10$.

In all cases apart from $N = 9$, only one solution is stable for $\delta < 10^{-3}$ and a stable fixed point loses stability through a supercritical Hopf bifurcation as $\delta$ is decreased, and the resulting periodic orbit then becomes chaotic after period-doubling. The $N = 9$ case seems to be the transition between the T2 solution being stable for $\delta = 10^{-3}$ and then destabilising as $\delta$ is decreased ($N < 9$), and

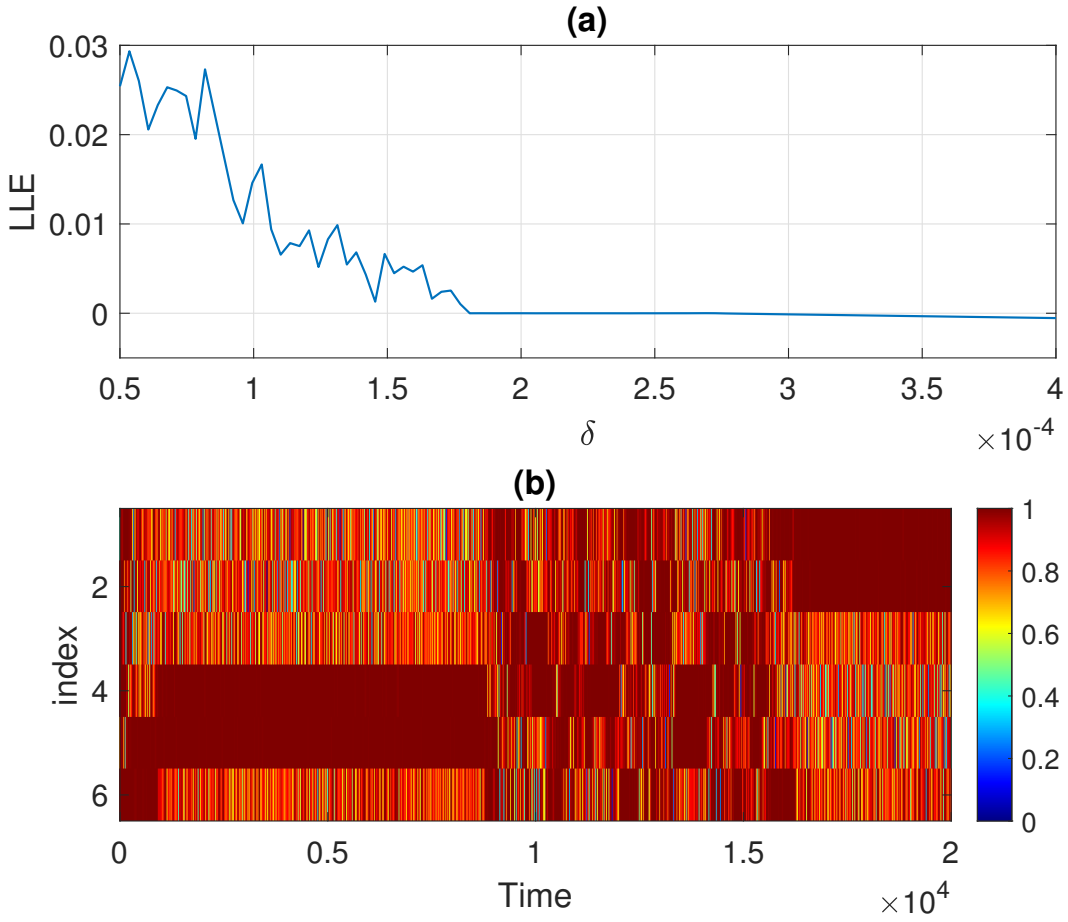


FIG. 10. $N = 6$. (a): largest Lyapunov exponent (LLE) as a function of $\delta$. (b): a typical solution for $\delta = 10^{-4}$. $|z|$ is plotted in colour.

the T1 solution undergoing these transitions ($N > 9$). The reason for this transition at $N = 9$ is unknown.

While we cannot explore all of phase space, we found that for $5 \leq N \leq 8$, for which a T1 solution was unstable for $0 < \delta \leq 10^{-3}$, an initial condition near such a state was attracted to a T2 solution. Similarly, for $10 \leq N \leq 12$, for which a T2 solution was unstable, an initial condition near such a state was attracted to a T1 solution.

The results above for $N = 2, 3 \ldots, 12$ were verified in finite populations with $M = 50$. For $N > 5$ the chaotic wandering of the chimera around the domain was observed for sufficiently small $\delta$.

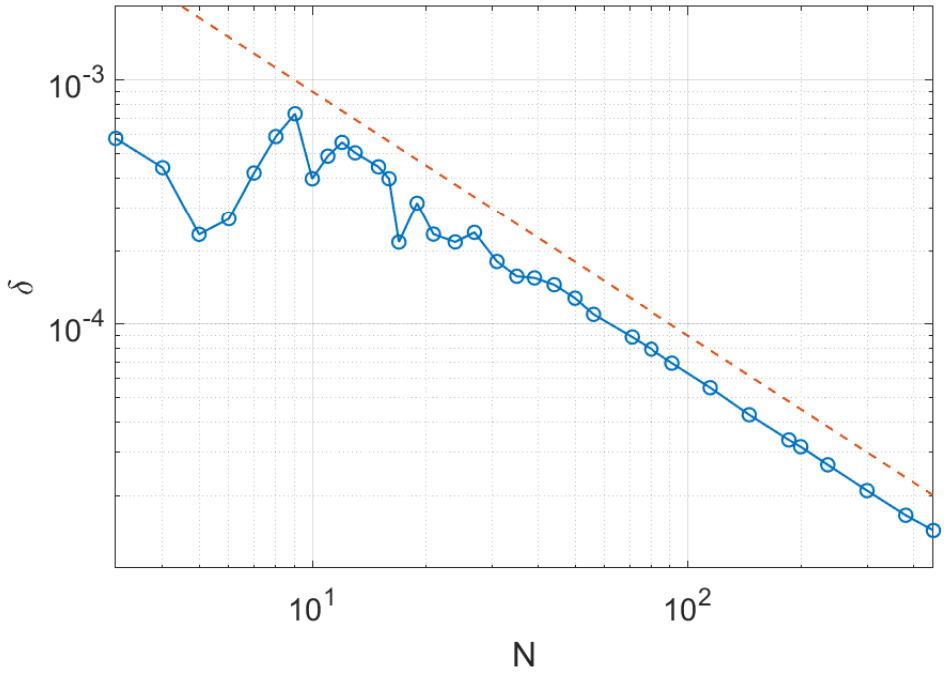


FIG. 11. Value of $\delta$ at which a stationary chimera loses stability through a Hopf bifurcation. (For $N = 4$ the T1 solution was followed.) The chimera is stable above the curve. The dashed line indicates the scaling $\delta \sim N^{-1}$.

## B. Varying $N$ and $\delta$

For selected values of $N$ in the interval $[3,450]$ we integrated (11)-(12) to a steady state at $\delta = 10^{-3}$ and then followed this state using pseudo-arclength continuation as $\delta$ was decreased[11,17]. We recorded the value of $\delta$ at which the state became unstable through a Hopf bifurcation and these values are shown on a log-log scale in Fig. 11. While there are some fluctuations for small $N$, it seems that for larger $N$ this value of $\delta$ scales as $N^{-1}$ (dashed line in Fig. 11), implying that instability is a finite-population effect which does not occur for the continuum case (7)-(8).

We also calculated the largest Lyapunov exponent, quasistatically decreasing $\delta$, for values of $N$ ranging from 3 to 30 inclusive. The results are shown in Fig. 12. We see that $N = 6$ is the smallest network for which chaotic behaviour occurs, and the value of $\delta$ below which the system is chaotic decreases with $N$ for large $N$. The results in Fig. 11 imply that this chaotic behaviour is also a finite-population effect.

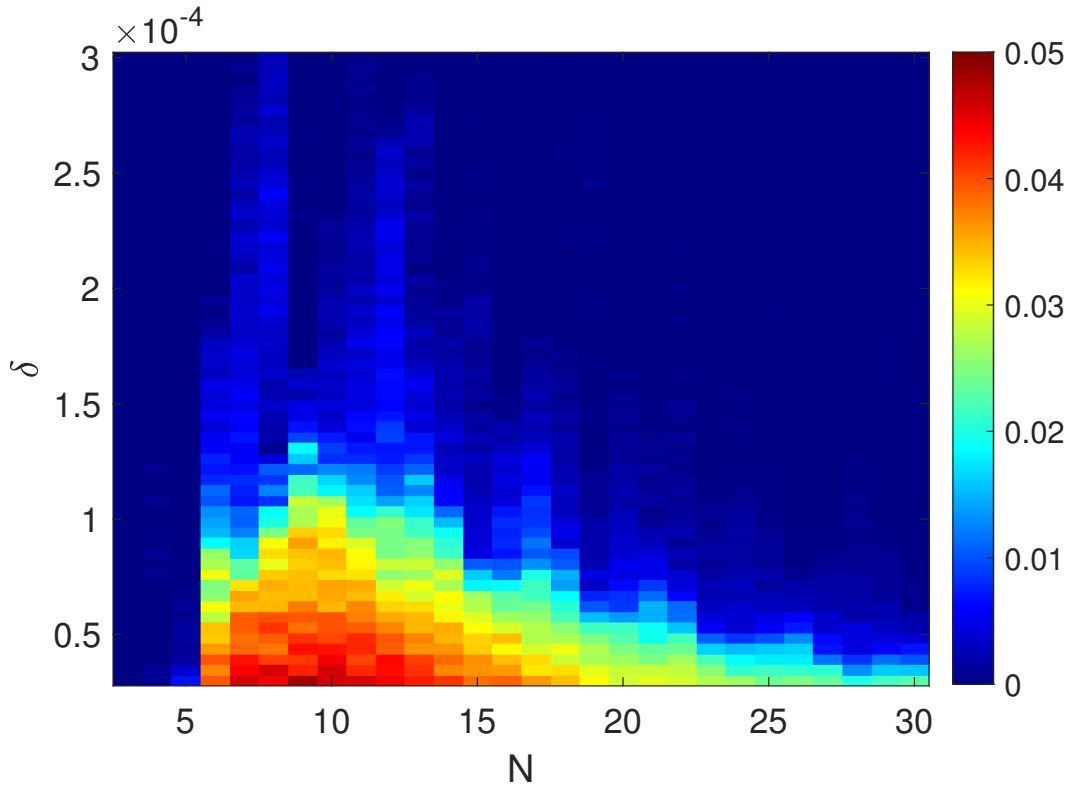


FIG. 12. Largest Lyapunov exponent (colour) as both $N$ and $\delta$ are varied.

### C. Stability of the equally-synchronous state

One characteristic of chimeras is that they are often stable for parameter values for which the fully synchronous state is also stable, although this is not always the case, particularly for heterogeneous networks[12,14]. The equally-synchronous state is a fixed point of (11)-(12) for which $r_k = \rho$ for $k = 1, 2, \ldots N$ and all $\psi_k = 0$. $\rho = 0$ is always a fixed point, corresponding to complete incoherence, but there is a non-zero solution of this form for which

$$\rho = \sqrt{1 - \frac{2\delta}{\sin\beta}} \tag{26}$$

for $0 \leq \delta < \sin(\beta)/2 \approx 0.014998$ for $\beta = 0.03$. Following this state for various $N$ we find it is stable for $\delta = 0$ (corresponding to perfect synchrony) but becomes unstable as $\delta$ is increased, before stabilising again at $\delta \approx 4 \times 10^{-3}$; see Fig. 13. Thus there are regions of parameter space for which it seems that a chimera is the only attractor. This is consistent with our observations above that when starting near an unstable T1 (T2) chimera, the system was attracted to a stable T2 (T1) chimera, rather than to the synchronous state.

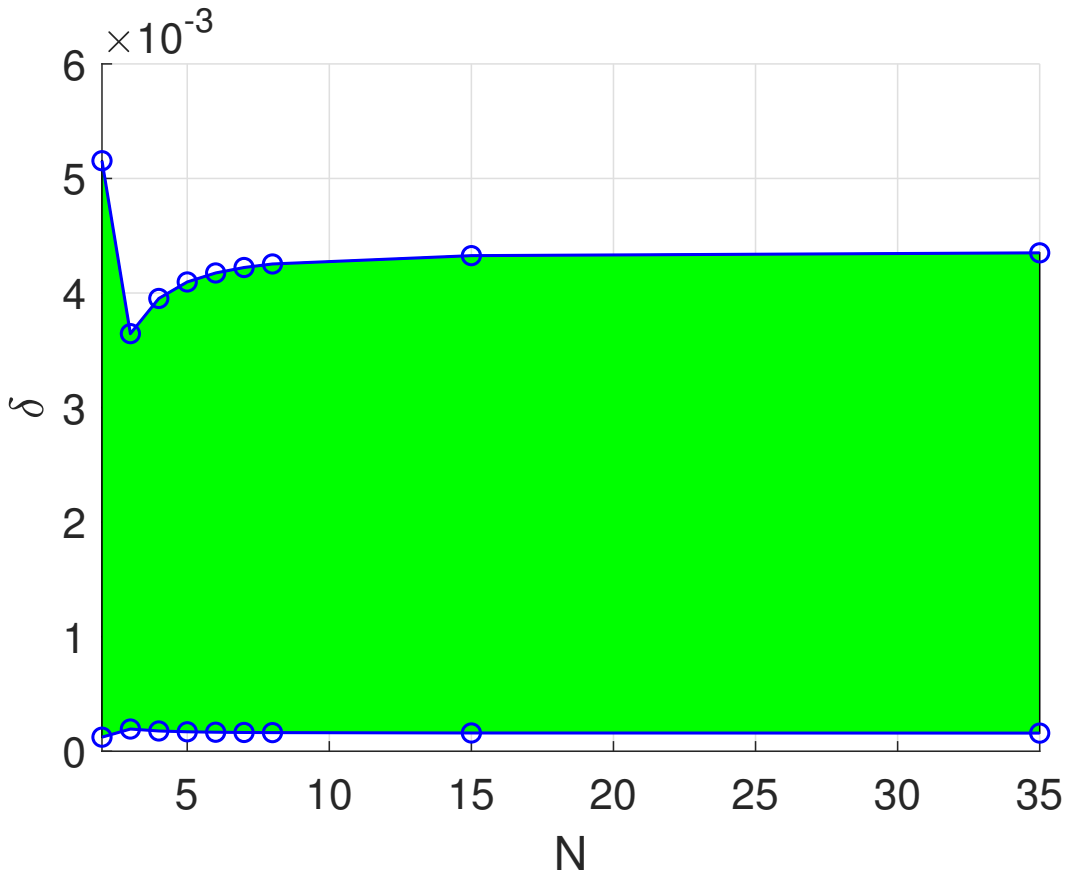


FIG. 13. The equally-synchronous state is *unstable* in the coloured region.

## IV. DISCUSSION

We studied a network formed from $N$ infinite populations of oscillators equally spaced around a ring, with nonlocal coupling between populations. We obtained the same results as previous authors for $N = 2$, and for $N = 3$ showed that one of the types of chimera observed by Martens[19] is not actually stable, at least for infinite populations. For each $N \in \{4, \ldots 12\}$ we found that at most two types of stable chimeras exist for small levels of frequency heterogeneity, and they all have the form of a coarse-grained version of that which occurs in the spatially continuous system[2,3,15,22]. All of the stable solutions of this form become unstable through a supercritical Hopf bifurcation as $\delta$ is decreased, and the resulting periodic solution then becomes unstable through either a Neimark-Sacker bifurcation ($N = 4, 5$) or period-doubling leading to chaotic behaviour ($6 \leq N \leq 12$). This phenomenon of chaotic behaviour requiring sufficiently many populations was observed in[10], who studied Kuramoto oscillators with inertia. Chaotic behaviour was also observed by Bick

et al.[6] in a network of two populations, but with different phase lag parameters (our $\alpha$) for coupling within a population and between populations. "Turbulence" was also observed in the continuum limit ($N \to \infty$) equations for some values of the phase lag[7–9,33].

We found that the value of $\delta$ at which a stable stationary chimera loses stability in a Hopf bifurcation decreases as $\sim N^{-1}$ as $N$ increases, suggesting that the observed oscillatory behaviour for finite $N$ vanishes as $N \to \infty$, along with the observed chaotic behaviour. Our results help bridge the gap between the well-studied $N = 2$ case[1,12,14,16,26] and the $N = \infty$ case [2,3,15,22]. We observed similar results holding $B = 0.35$ and choosing $\beta = 0.05$ (rather than $\beta = 0.03$), and also for $B = 0.25$ and $\beta = 0.03$, suggesting that our results are generic, at least for small $\beta$.

## REFERENCES


[1]D.M. Abrams, R. Mirollo, S.H. Strogatz, and D.A. Wiley. Solvable model for chimera states of coupled oscillators. *Phys. Rev. Lett.*, 101(8):084103, 2008.

[2]D.M. Abrams and S.H. Strogatz. Chimera states for coupled oscillators. *Phys. Rev. Lett.*, 93(17):174102, 2004.

[3]D.M. Abrams and S.H. Strogatz. Chimera states in a ring of nonlocally coupled oscillators. *Int. J. Bifurcat. Chaos*, 16(1):21–37, 2006.

[4]Gilad Barlev, Thomas M. Antonsen, and Edward Ott. The dynamics of network coupled phase oscillators: An ensemble approach. *Chaos*, 21(2):025103, 2011.

[5]E. Barreto, B. Hunt, E. Ott, and P. So. Synchronization in networks of networks: The onset of coherent collective behavior in systems of interacting populations of heterogeneous oscillators. *Phys. Rev. E*, 77(3):036107, 2008.

[6]Christian Bick, Mark J Panaggio, and Erik A Martens. Chaos in kuramoto oscillator networks. *Chaos: An Interdisciplinary Journal of Nonlinear Science*, 28(7):071102, 2018.

[7]Maxim Bolotov, Lev Smirnov, Grigory Osipov, and Arkady Pikovsky. Simple and complex chimera states in a nonlinearly coupled oscillatory medium. *Chaos: An Interdisciplinary Journal of Nonlinear Science*, 28(4):045101, 2018.

[8]MI Bolotov, LA Smirnov, ES Bubnova, GV Osipov, and AS Pikovsky. Spatiotemporal regimes in the kuramoto–battogtokh system of nonidentical oscillators. *Journal of Experimental and Theoretical Physics*, 132(1):127–147, 2021.

[9]Grigory Bordyugov, Arkady Pikovsky, and Michael Rosenblum. Self-emerging and turbulent

chimeras in oscillator chains. *Physical Review E*, 82(3):035205, 2010.

[10]Barrett N. Brister, Vladimir N. Belykh, and Igor V. Belykh. When three is a crowd: Chaos from clusters of kuramoto oscillators with inertia. *Phys. Rev. E*, 101:062206, Jun 2020.

[11]Willy JF Govaerts. *Numerical methods for bifurcations of dynamical equilibria*, volume 66. Siam, 2000.

[12]Tejas Kotwal, Xin Jiang, and Daniel M Abrams. Connecting the kuramoto model and the chimera state. *Physical review letters*, 119(26):264101, 2017.

[13]Y. Kuramoto and D. Battogtokh. Coexistence of Coherence and Incoherence in Nonlocally Coupled Phase Oscillators. *Nonlinear Phenom. Complex Syst*, 5(4):380–385, 2002.

[14]Carlo R. Laing. Chimera states in heterogeneous networks. *Chaos*, 19(1):013113, 2009.

[15]Carlo R. Laing. The dynamics of chimera states in heterogeneous Kuramoto networks. *Physica D*, 238(16):1569–1588, 2009.

[16]Carlo R Laing. Disorder-induced dynamics in a pair of coupled heterogeneous phase oscillator networks. *Chaos*, 22(4):043104, 2012.

[17]Carlo R Laing. Numerical bifurcation theory for high-dimensional neural models. *The Journal of Mathematical Neuroscience*, 4(1):13, 2014.

[18]Carlo R Laing, Karthikeyan Rajendran, and Ioannis G Kevrekidis. Chimeras in random non-complete networks of phase oscillators. *Chaos*, 22(1):013132, 2012.

[19]Erik A. Martens. Bistable chimera attractors on a triangular network of oscillator populations. *Phys. Rev. E*, 82:016216, Jul 2010.

[20]E. Montbrió, J. Kurths, and B. Blasius. Synchronization of two interacting populations of oscillators. *Phys. Rev. E*, 70(5):056125, 2004.

[21]O E Omel'chenko. The mathematics behind chimera states. *Nonlinearity*, 31(5):R121–R164, apr 2018.

[22]Oleh E Omel'chenko. Coherence–incoherence patterns in a ring of non-locally coupled phase oscillators. *Nonlinearity*, 26(9):2469, 2013.

[23]Edward Ott and Thomas M. Antonsen. Low dimensional behavior of large systems of globally coupled oscillators. *Chaos*, 18(3):037113, 2008.

[24]Edward Ott and Thomas M. Antonsen. Long time evolution of phase oscillator systems. *Chaos*, 19(2):023117, 2009.

[25]Mark J Panaggio and Daniel M Abrams. Chimera states: coexistence of coherence and incoherence in networks of coupled oscillators. *Nonlinearity*, 28(3):R67, 2015.

[26]Mark J Panaggio, Daniel M Abrams, Peter Ashwin, and Carlo R Laing. Chimera states in networks of phase oscillators: the case of two small populations. *Physical Review E*, 93(1):012218, 2016.

[27]A. Pikovsky and M. Rosenblum. Partially integrable dynamics of hierarchical populations of coupled oscillators. *Phys. Rev. Lett.*, 101(26):264103, 2008.

[28]Arkady Pikovsky and Michael Rosenblum. Dynamics of heterogeneous oscillator ensembles in terms of collective variables. *Physica D: Nonlinear Phenomena*, 240(9):872–881, 2011.

[29]P.S. Skardal and J.G. Restrepo. Hierarchical synchrony of phase oscillators in modular networks. *Physical Review E*, 85(1):016208, 2012.

[30]L. A. Smirnov, G. V. Osipov, and A. Pikovsky. Solitary synchronization waves in distributed oscillator populations. *Phys. Rev. E*, 98:062222, Dec 2018.

[31]Lev Smirnov, Grigory Osipov, and Arkady Pikovsky. Chimera patterns in the kuramoto–battogtokh model. *Journal of Physics A: Mathematical and Theoretical*, 50(8):08LT01, 2017.

[32]S. Watanabe and SH Strogatz. Constants of motion for superconducting Josephson arrays. *Physica D*, 74:197–253, 1994.

[33]Matthias Wolfrum, Svetlana V Gurevich, and Oleh E Omel'chenko. Turbulence in the ott–antonsen equation for arrays of coupled phase oscillators. *Nonlinearity*, 29(2):257, 2016.

[34]Matthias Wolfrum and E Omel'chenko. Chimera states are chaotic transients. *Physical Review E*, 84(1):015201, 2011.

[35]Jianbo Xie, Edgar Knobloch, and Hsien-Ching Kao. Multicluster and traveling chimera states in nonlocal phase-coupled oscillators. *Physical Review E*, 90(2):022919, 2014.